Reproductive Biology and Endocrinology

RESEARCH

Open Access

Changes in the interactions between mural granulosa cells and cumulus cells during ovulation after the LH surge based on transcriptome analyses

Amon Shiroshita[1], Isao Tamura[1*], Marina Ito[1], Toshihide Yoneda[1], Hitomi Takasaki-Kawasaki[1], Taishi Fujimura[1], Yuichiro Shirafuta[1], Toshiaki Taketani[1], Shun Sato[1] and Norihiro Sugino[1]

Abstract

Background The luteinizing hormone (LH) surge during ovulation induces dynamic changes in cellular functions of mural granulosa cells (MGCs) and cumulus cells (CCs). However, the mechanisms by which the two cell types interact with each other and regulate their cellular functions remain unclear. In this study, we investigated transcriptomic changes in both cell types in order to reveal the cell-cell interactions between MGCs and CCs during the ovulatory process.

Methods MGCs and CCs were collected from mice treated with equine chorionic gonadotropin (eCG), at 0 h (before), and 4 and 12 h after human chorionic gonadotropin (hCG) injection. Transcriptomes of both cell types were obtained by RNA sequencing. The changes in cellular functions and cell-cell interactions were investigated by gene ontology (GO) analysis and interactome analysis, respectively. To validate the predicted interactions, MGCs and COCs collected 48 h after eCG injection were cocultured for 12 h, after which gene expression and COC expansion were assessed.

Results From 0 to 4 h after hCG injection, many cellular functions, including steroidogenesis, angiogenesis, follicle rupture, inflammatory response and cumulus-oocyte complex (COC) expansion were activated by cell-cell interactions, most of which were bidirectional interactions between MGCs and CCs. From 4 h to 12 h, cell-cell interactions regulating angiogenesis, follicle rupture, and inflammatory response remained activated, while those regulating steroidogenesis and COC expansion were attenuated. The coculture model revealed that COC expansion was induced in the presence of MGCs. Furthermore, the expressions of genes related to steroidogenesis, angiogenesis, and COC expansion in CCs increased in the presence of MGCs while their expressions in MGCs increased in the presence of CCs.

Conclusions Interactions between MGCs and CCs regulate the dynamic and time-dependent changes in their cellular functions during the ovulatory process, highlighting their essential regulatory roles.

Keywords Ovary, Mural granulosa cell, Cumulus cell, Cell interaction, Ovulation, Luteinization

*Correspondence:
Isao Tamura
isao@yamaguchi-u.ac.jp
[1]Department of Obstetrics and Gynecology, Yamaguchi University Graduate School of Medicine, Minamikogushi 1-1-1, Ube 755-8505, Japan

Background

Ovarian granulosa cells differentiate into two distinct populations during follicular antrum formation: mural granulosa cells (MGCs), which line the follicular wall, and cumulus cells (CCs), which surround the oocyte and form the cumulus-oocyte complex (COC). The ovulatory luteinizing hormone (LH) surge induces dramatic changes in various cellular functions, including steroidogenesis, angiogenesis, follicle rupture, and inflammatory response in MGCs undergoing ovulation [1–4]. The LH surge also induces cellular functional changes in CCs, such as oocyte maturation and COC expansion [5, 6]. These functional changes in both cell types contribute to ovulation and corpus luteum formation. LH receptors are strongly expressed in MGCs but weakly expressed in CCs [7]. Therefore, MGCs can directly respond to the LH surge, while CCs depend on indirect signaling mediated by MGCs [8]. Although some of the actions of MGCs on CCs have been identified [9, 10], detailed interactions between MGCs and CCs are not fully understood. It is especially unclear whether CCs have actions on MGCs. There is thus a need for a better understanding of the interactions between the two cell types and their involvement in cellular functions during ovulation. We have recently identified potential interactions between the two cell types by performing a pseudo-time analysis using mouse ovary single-cell RNA-sequence data [11, 12]. However, this analysis was somewhat speculative because it was based on an in silico approach using transcriptome data from a single time point during ovulation and thus might not adequately capture changes in interactions during the in vivo ovulatory process. In this study, we obtained transcriptome data of MGCs and CCs from three time points during ovulation and investigated the interactions between the two cell types and their involvement in cellular functions. In addition, there has not been an appropriate in vitro model to examine the interactions between MGCs and CCs. Therefore, establishing a coculture model that recapitulates these interactions during the ovulatory process is essential. In this study, in addition to a comprehensive analysis of interactions based on transcriptome data, we established an in vitro coculture model of MGCs and CCs, which enabled us to validate their interactions during ovulation.

Materials and methods

Isolation of mural granulosa cells and cumulus cells

This study was reviewed and approved by the committee for ethics on animal experiment in Yamaguchi University Graduate School of Medicine. All experiments were performed in accordance with relevant guidelines and regulations. C57BL/6 female mice (aged 21days) were purchased from Japan SLC. They were injected intraperitoneally with 4 IU of equine chorionic gonadotropin (eCG) (Aska Animal Health) to promote follicular growth. After 48 h, 5 IU of human chorionic gonadotropin (hCG) (Sigma-Aldrich) was injected to induce ovulation. The ovaries were obtained before (0), and 4 and 12 h after hCG injection. This time-point was based on our previous reports showing that gene expression levels of *StAR*, *Cyp11a1*, and *Cyp19a1* dramatically change in the 0–4 h and 4–12 h phases in rat and mouse MGCs [1, 13, 14]. The follicles were punctured to isolate MGCs and COCs. COCs were collected using a fine-bore Pasteur pipette under a stereomicroscope. After removing COCs, the punctured ovarian tissues were discarded, and the remaining follicular cells were collected as MGCs by centrifugation (3000 rpm, 10 min) and used for quantitative Reverse Transcriptase–Polymerase Chain Reaction (qRT-PCR), and RNA sequencing (RNA-seq). To isolate CCs, COCs were washed and transferred using the micropipettes into 250μL of individual droplet containing 0.01% of hyaluronidase (Sigma-Aldrich). Oocytes were freed from surrounding CCs by gentle pipetting with a 75 μm micropipette. Denuded oocytes were carefully removed, and the remaining dispersed cells were collected by centrifugation (3000 rpm, 10 min) and used as CCs for qRT-PCR, and RNA-seq. Although a few follicles ovulated at 12 h, most of the MGCs and COCs used in this study were from the preovulatory follicles. To collect postovulatory COCs, the oviducts were removed and COCs were isolated. To collect postovulatory MGCs, postovulatory follicles were punctured to release MGCs. The collected COCs and MGCs were processed as described above. The mean numbers of cells collected from one mouse at each time point were as follows: MGCs, 0 h: 2.3×10^6, 4 h: 2.2×10^6, 12 h: 1.6×10^6; CCs, 0 h: 4.8×10^4, 4 h: 3.3×10^4, 12 h: 4.1×10^4.

Quantitative reverse transcriptase–polymerase chain reaction (qRT-PCR)

A total of 80 ng of RNA from CCs and 400 ng of RNA from MGCs were reverse transcribed using ReverTra Ace® qPCR RT Master Mix (Toyobo) according to the manufacturer's instructions. Real-time RT-PCR was performed on a CFX384 Touch Real-Time PCR Detection System (Bio-Rad) using Luna® Universal qPCR Master Mix (New England Biolabs) as reported previously [15–17]. The PCR cycling conditions were as follows: initial denaturation at 95 °C for 1 min, followed by 45 cycles of denaturation at 95 °C for 5 s and annealing/extension at 60 °C for 20 s. Melt-curve analysis was performed to verify the specificity of amplification. Gapdh was used as the internal control. Primer sequences, annealing temperature, and product size are listed in Supplementary Table 1.

RNA sequencing (RNA-seq)

Total RNA was isolated from MGCs and CCs from 3 mice at each time point (0, 4, and 12 h after hCG injection), with RNeasy® Mini Kit (Qiagen) and RNeasy Micro Kit (Qiagen), respectively, 1221 ~ 4251 ng from MGCs and 44 ~ 294 ng from CCs, which were sufficient for RNA sequencing. Before proceeding to RNA-seq, we confirmed by qRT-PCR that messenger RNA (mRNA) expression of the representative genes that alter in MGCs after the LH surge (*StAR*, *Cyp11a1*, *and Cyp19a1*) [1, 13, 14] showed similar time-course patterns as reported previously (Supplementary Fig. 1). At each of 3 time points, RNA samples from 2 to 3 mice were mixed, and 20 ng of RNA from CCs and 100 ng of RNA from MGCs were used for RNA-seq analysis. RNA-seq was performed as we reported previously [1, 15]. The mRNA-sequence library was generated and was sequenced on NovaSeq 6000 platform (Illumina). Mapping and quantification of gene expression were performed by CLC Genomics Workbench with default settings.

Differential expression and gene ontology analysis

Differential expression analysis of gene counts was implemented by an R package "DESeq2" (v.1.42.0) as reported previously [18]. A negative binomial generalized linear regression model was used to fit the RNA-seq data, and Wald tests were performed to detect the significant differentially expressed genes (DEGs) based on 3 biologic replicates of each condition. The resulting P-values were adjusted by the Benjamini-Hochberg procedure for multiple comparisons. We set the adjusted P-value threshold at 1% using the Benjamini–Hochberg method in order to minimize false positives and to obtain a more robust set of differentially expressed genes. Given the large number of genes examined in RNA-seq analysis, a stricter cutoff was chosen to ensure reliability of downstream GO analyses. The genes whose expression values increased or decreased between 2 time points (0 h vs. 4 h or 4 h vs. 12 h) more than 1.5-log2 fold change or less than – 1.5-log2 fold change were defined as upregulated or downregulated genes, respectively. We reported that a number of genes show transient increases or decreases at 4 h after hCG stimulation [1]. The aim of the present study was to investigate in detail the dynamic and short-term changes of genes and interactions during the ovulatory process. Therefore, we focused on comparisons between 0 h and 4 h, and 4 h and 12 h, which we considered most appropriate to capture such transient changes. DAVID Bioinformatics Resources v.6.8 (https://david.ncifcrf.gov/) was used to determine whether the functional annotation of the DEGs was enriched for specific Gene Ontology (GO) terms [19]. P-values less than 0.05 were considered to indicate significant enrichment. Then, the GO terms were summarized by removing redundancy and plotted using reduce and visualize gene ontology (REVIGO) with allowed similarity as "Tiny (0.3)" [20].

Interactome analysis

To investigate the interactions between MGCs and CCs during ovulation, interactome analysis was performed, as reported previously [11, 21]. Given that cell numbers can affect interactome analysis, we augmented the number of MGCs and CCs. The augmented cell numbers were determined based on the detected counts from publicly available murine ovarian single-cell transcriptomic datasets [12]. According to the expression of the established marker genes, each cell population was defined as follows: MGCs (Snap25), CCs (Ube2c) [11, 12]. A total of 680 MGCs and 312 CCs were detected in the mouse ovary (Supplementary Fig. 2). These numbers were used to augment the bulk RNA, increasing MGCs from 3 to 680 cells and CCs from 3 to 312 cells, with the addition of 0.1% of Gaussian noise [22]. The augmented RNA-seq data were converted into feature barcode matrices, which were imported using Read10x function and CreateSeuratObject function in Seurat (version 5.2.1) [23]. Gene expression levels were calculated as log-transformed counts using NormalizeData. Interactome analysis was performed using CellChat (version 1.1.3) [21] with customized parameters, including selection of the "Secreted Signaling" category, as the interaction between MGCs and CCs was considered to be mediated by secreted signaling. The strength of cell-cell interaction was calculated by "Communication Probability" [21]. We added 1.0×10^{-5} to the Communication Probability value before the following calculation. To extract effective interactions between MGCs and CCs, we used the value of Communication Probability. Since in our dataset, previously reported interactions from MGCs to CCs (e.g., Nppc→Npr2 and Btc→ERBB2_ERBB4) [9, 10] showed Communication Probability values of approximately 0.01, we set the Communication Probability threshold at 0.01. We compared the Communication Probability of actions between the 0–4 h phase and 4–12 h phase. The actions whose Communication Probability increased by > 2-fold or decreased to < 0.5-fold between 0 h vs. 4 h and 4 h vs. 12 h were identified as "activated action" or "attenuated action", respectively. The involvement of activated or attenuated actions in the cellular functional changes were identified by in silico analysis. Activated actions were considered to influence the cellular functional changes derived from upregulated genes, while attenuated actions were considered to influence the cellular functional changes derived from downregulated genes. Additionally, any actions of MGCs on CCs were considered to affect the cellular functions of CCs, while any actions of CCs on MGCs were considered to affect the cellular functions of MGCs.

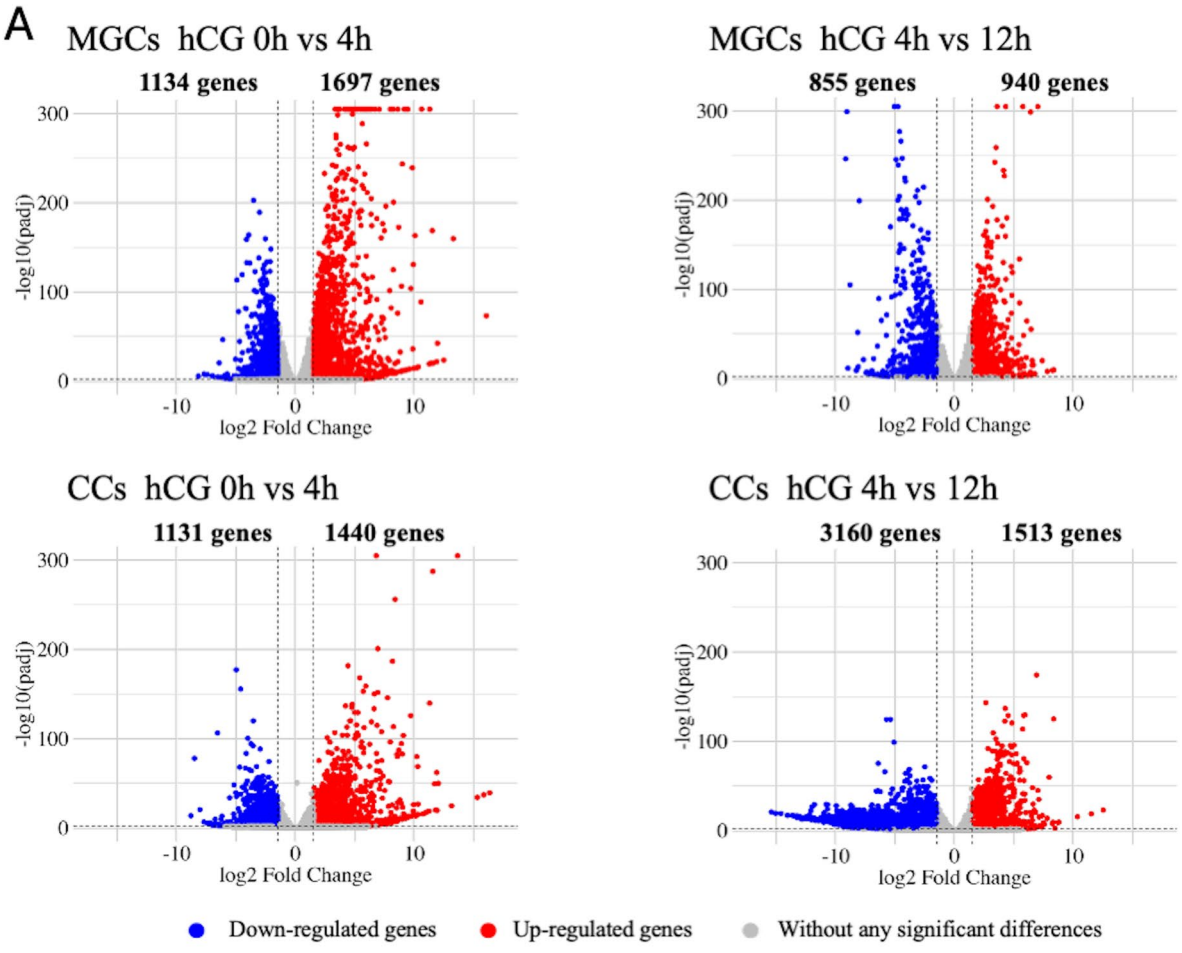

Fig. 1 (See legend on next page.)

(See figure on previous page.)

Fig. 1 Changes in genome-wide gene expression in MGCs and CCs during ovulation. **A** Volcano plots are depicted with the fold change of each gene and the P-value was calculated by performing a Wald test and adjusted by Benjamini-Hochberg procedure. DEGs were identified by comparing the transcriptomes between 0 h vs. 4 h, and 4 h vs. 12 h, respectively. More than 1.5-log2 fold change or less than −1.5-log2 fold change were defined as upregulated or downregulated genes. Adjusted P-values threshold were set as 1%. Blue dots show downregulated genes. Red dots show upregulated genes. Gray dots show genes without any significant differences. **B** Venn diagrams showing differentially expressed genes in MGCs (top) and CCs (bottom) after hCG injection. Comparisons were made between 0 h vs. 4 h and 4 h vs. 12 h. Left panels show upregulated genes (red arrows), and right panels show downregulated genes (blue arrows)

In vitro coculture of MGCs and COCs

Ovaries of immature mice (3 weeks old) were obtained at 48 h after eCG injections. MGCs were collected as described in "Isolation of mural granulosa cells and cumulus cells" Sect. 1.5×10^5 cells/well were seeded onto the bottom chamber of a fetal calf serum (FCS)-recoated 96-well plate (HTS Transwell-96 Permeable Support with 8.0-mm Pore Polyester Membrane no. 3374; Corning Incorporated) with DMEM/F12 Medium (Nacalai Tesque). COCs were also collected from the same mice as described in the same section. Since CCs lose their characteristic features without the presence of an oocyte [24], they were cultured in the form of COCs. 50 COCs per well were seeded onto the upper insert of the plate with DMEM/F12 Medium. To recapitulate and examine the actions of MGCs on CCs during ovulation, 2 IU/mL hCG (Sigma-Aldrich) was added to the culure medium to stimulate MGCs. Since CCs do not directly respond to hCG [9], 100 ng/mL amphiregulin (Areg; R&D Systems) was added to the culure medium to examine the actions of CCs on MGCs during ovulation, as reported previously [9]. To validate the actions of MGCs on CCs, COCs were cultured either without hCG (control), with hCG, or cocultured with MGCs in the presence of hCG. To validate the actions of CCs on MGCs, MGCs were cultured either without Areg (control), with Areg, or cocultured with COCs in the presence of Areg. After 12 h of culture, COC expansion was observed. In addition, MGCs and CCs isolated from COCs were subjected to qRT-PCR analysis to evaluate whether the two cell types influenced each other.

Statistical analysis

Differences between groups were analyzed by one-way analysis of variance followed by a Tukey-Kramer test. All statistical analyses were performed using R (version 4.3.2, R Foundation for Statistical Computing, Vienna, Austria). Differences were considered significant at P-values less than 0.05.

Results

Changes in genome-wide gene expression in MGCs and CCs during ovulation

To investigate the changes in genome-wide gene expression during ovulation, we performed RNA-seq of MGCs and CCs at 3 time points, before (0 h) and 4 h and 12 h after hCG injection. Thousands of differentially expressed genes (DEGs) were identified during the first 4 h and the following 12 h in the two cell types (Fig. 1A). In MGCs, 1697 genes were upregulated, and 1134 genes were downregulated from 0 h to 4 h. From 4 h to 12 h, 940 genes were upregulated, and 855 genes were downregulated. In CCs, 1440 genes were upregulated, and 1131 genes were downregulated from 0 h to 4 h. From 4 h to 12 h, 1513 genes were upregulated, and 3160 genes were downregulated. All DEGs are listed in Supplementary Table 2. Venn diagrams indicated that a subset of DEGs was shared between the comparisons of 0 h vs. 4 h and 4 h vs. 12 h (Fig. 1B).

Changes in cellular functions of MGCs and CCs during ovulation

GO analysis was performed to identify the cellular functions associated with the DEGs (Supplementary Table 3). The enriched GO terms were summarized by REVIGO analysis [20] and classified into 20 representative cellular functions (Fig. 2, orange column). Figure 2 shows changes in cellular functions of MGCs and CCs during ovulation. Both MGCs and CCs exhibited dramatic changes in cellular functions during ovulation, indicating that many of these functional changes and physiological processes were driven by extensive gene up- or down-regulation in both MGCs and CCs. In CCs, 'oocyte maturation' was uniquely identified, highlighting a cell-type–specific function, whereas other functions were observed in both MGCs and CCs. This suggests that, although MGCs and CCs retain distinct roles, they also undergo overlapping functional changes during the ovulatory process.

Changes in cell–cell interactions between MGCs and CCs during ovulation

We hypothesized that the dramatic changes in cellular functions of MGCs and CCs (Fig. 2, Supplementary Table 4) are regulated by cell-cell interactions between them. To identify the interactions between MGCs and CCs during ovulation, an interactome analysis was performed using RNA-seq data. To extract effective interactions between MGCs and CCs, we set a communication probability threshold of 0.01 and selected interactions exceeding this threshold at any time point (Supplementary Table 5). These were defined as "action" that shows an interaction between MGCs and CCs. For example, if MGCs highly express ligand A or CCs highly express a receptor for ligand A, this is referred to an action of

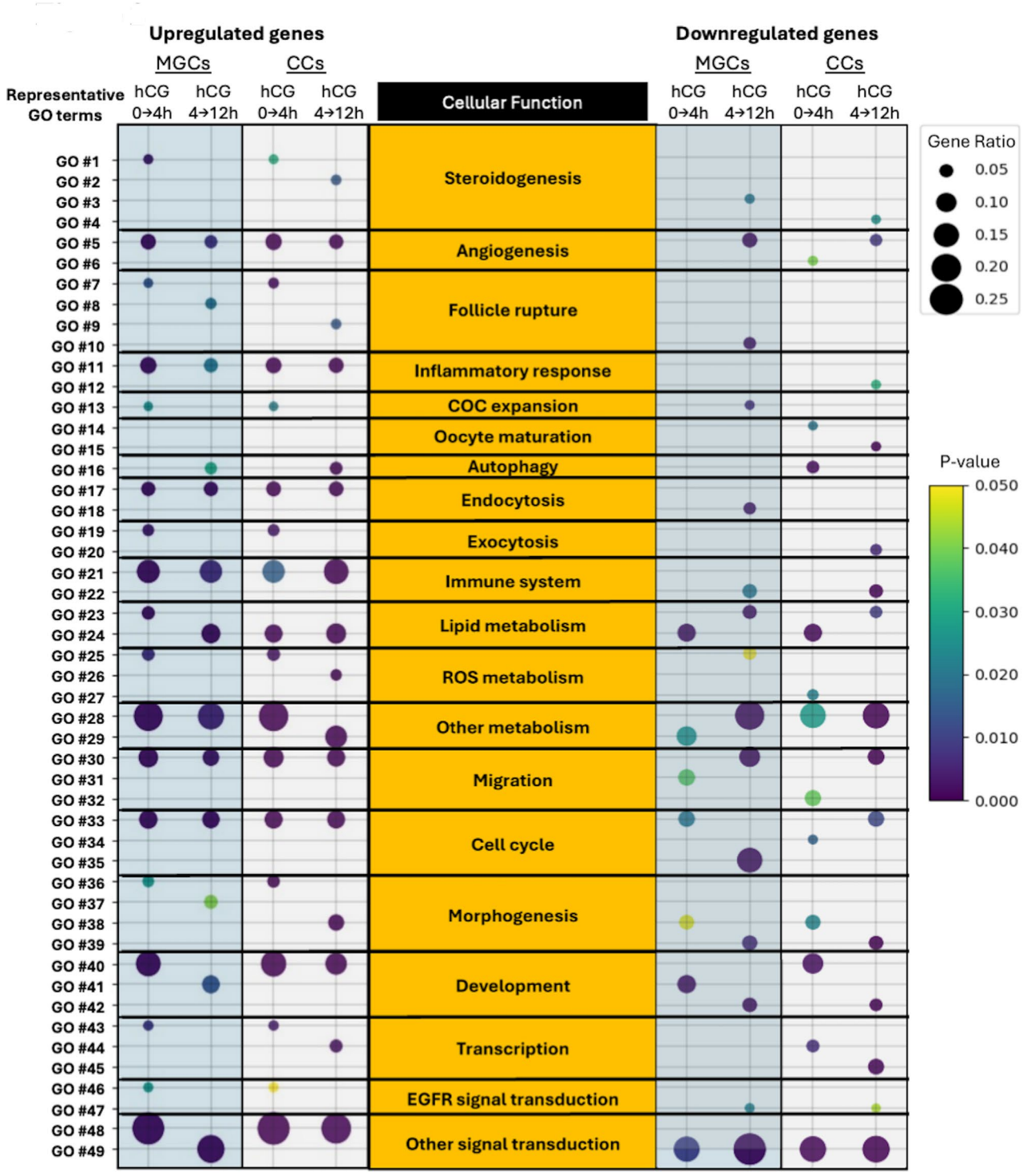

Fig. 2 Changes in cellular functions of MGCs and CCs during ovulation. The up or downregulated genes in MGCs and CCs were subjected to GO-REVIGO analysis, respectively. The cellular functions are shown in the orange column and their corresponding GO terms are shown on the left with numbers (see Table 1 for the full GO terms). The figure is based on gene ratios which are defined as the ratio of DEGs to all genes in each GO term. The gene ratios are depicted as circles of different sizes and their P-values are indicated by color. A comprehensive list of the summarized GO terms and their associated cellular functions, along with their representative GO terms is given in Supplementary Table 4

Table 1 List of GO terms shown in Fig. 2

No.	representive GO term
GO #1	positive regulation of steroid biosynthetic process
GO #2	regulation of steroid biosynthetic process
GO #3	regulation of steroid hormone biosynthetic process
GO #4	regulation of steroid hormone secretion
GO #5	angiogenesis
GO #6	blood vessel remodeling
GO #7	ovulation
GO #8	regulation of muscle contraction
GO #9	ovulation cycle
GO #10	muscle contraction
GO #11	inflammatory response
GO #12	regulation of acute inflammatory response
GO #13	ovarian cumulus expansion
GO #14	negative regulation of oocyte maturation
GO #15	oocyte maturation
GO #16	regulation of autophagy
GO #17	endocytosis
GO #18	positive regulation of endocytosis
GO #19	regulation of exocytosis
GO #20	exocytosis
GO #21	immune system process
GO #22	negative regulation of immune system process
GO #23	regulation of lipid metabolic process
GO #24	lipid metabolic process
GO #25	response to oxidative stress
GO #26	reactive oxygen species metabolic process
GO #27	regulation of reactive oxygen species metabolic process
GO #28	positive regulation of metabolic process
GO #29	catabolic process
GO #30	cell migration
GO #31	cell motility
GO #32	regulation of cell motility
GO #33	cell death
GO #34	positive regulation of activated T cell proliferation
GO #35	regulation of cell population proliferation
GO #36	regulation of cell morphogenesis
GO #37	regulation of cytoskeleton organization
GO #38	cell morphogenesis
GO #39	actin filament-based process
GO #40	tissue development
GO #41	cell projection organization
GO #42	developmental maturation
GO #43	regulation of miRNA transcription
GO #44	regulation of DNA-binding transcription factor activity
GO #45	regulation of transcription by RNA polymerase II
GO #46	epidermal growth factor receptor signaling pathway
GO #47	ERBB2-EGFR signaling pathway
GO #48	signal transduction
GO #49	regulation of signaling

MGCs on CCs. We compared the communication probability of actions between the 0–4 h phase and 4–12 h phase. The actions whose Communication Probability increased by >2-fold or decreased to <0.5-fold between 0 h vs. 4 h and 4 h vs. 12 h were identified as "activated action" or "attenuated action", respectively (Fig. 3). The lower panel in Fig. 3 shows the number of activated and attenuated actions, categorized by direction (MGC→CC or CC→MGC) and time phase. For example, during the 0–4 h phase, 48 actions of MGCs on CCs were activated whereas 7 actions were attenuated. The number of the actions of CCs on MGCs (116 actions) was comparable to that of MGCs on CCs (108 actions) throughout the ovulation. In addition, the number of activated actions during the 0–4 h phase (96 actions) was much higher than during the 4–12 h phase (45 actions). Conversely, the number of attenuated actions was much higher during the 4–12 h phase (68 actions) than during the 0–4 h phase (15 actions). All activated and attenuated actions are shown in Supplementary Table 6.

Changes in cell-cell interactions and their association with physical phenomena during ovulation

To investigate the involvement of the identified interactions in the cellular functional changes during ovulation, the cellular functions identified by the GO analyses were combined with the interactions identified by interactome analyses (Fig. 4). For each action identified by the interactome analysis, we examined the ligand or receptor genes included in that action. Based on information from published literature, we determined the cellular functions in which these ligands or receptors are known to be involved. Activated actions were linked to functional changes associated with upregulated genes, whereas attenuated actions were linked to functional changes associated with downregulated genes. Any actions of MGCs on CCs were considered to affect the cellular functions of CCs, while any actions of CCs on MGCs were considered to affect the cellular functions of MGCs. For example, the interactome analysis identified Angptl2 as a ligand expressed in MGCs with its receptor in CCs, which was linked to inflammatory response, indicating that Angptl2 secreted from MGCs induces functional changes in CCs (inflammatory response) [25]. Conversely, the analysis also identified Fgf2 expressed in CCs with its receptor in MGCs, which was associated with steroidogenesis, indicating that Fgf2 secreted from CCs induces functional changes in MGCs (steroidogenesis). It also identified Tgfb1 expressed in CCs with its receptor in MGCs, which was associated with angiogenesis, indicating that Tgfb1 secreted from CCs induces functional changes in MGCs (angiogenesis). These represent novel interactions, as their involvement in the ovulatory process has not previously been reported. Figure

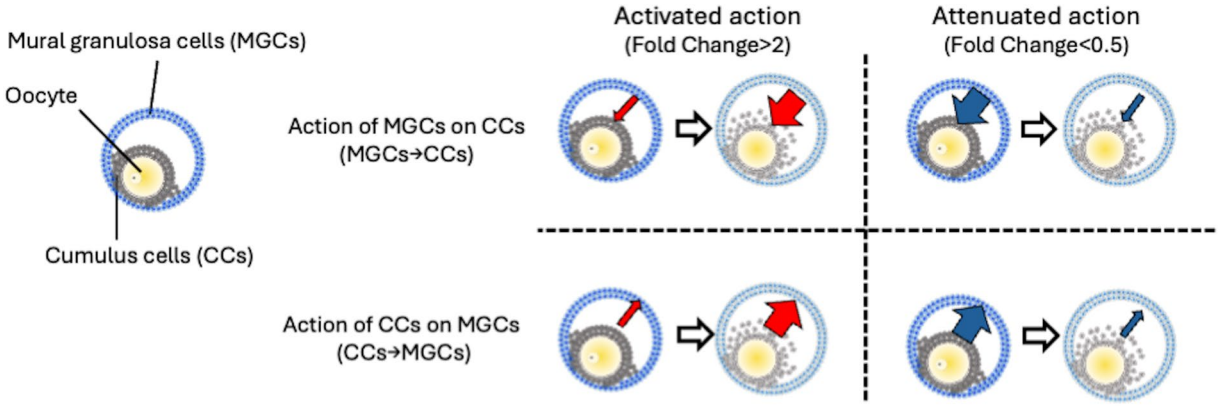

	Activated actions		Attenuated actions		
	hCG 0h→4h	hCG 4h→12h	hCG 0h→4h	hCG 4h→12h	Total
MGCs→CCs	48	18	7	35	108
CCs→MGCs	48	27	8	33	116
Total	96	45	15	68	

Fig. 3 The number of activated and attenuated actions during ovulation. The strength of cell-cell interaction was calculated by "Communication Probability" based on interactome analysis. The actions whose Communication Probability increased by > 2-fold or decreased to < 0.5-fold between 0 h vs. 4 h and 4 h vs. 12 h were identified as "activated action" or "attenuated action", respectively. The lower panel shows the number of activated and attenuated actions, categorized by direction (MGC→CC or CC→MGC) and time phase

4A shows cellular functions associated with upregulated genes and activated interactions. For example, during the 0–4 h phase, steroidogenesis was regulated by up-regulated genes in CCs and MGCs. Some actions involved in steroidogenesis worked bidirectionally between CCs and MGCs. During the 0–4 h phase, cellular functional changes derived from upregulated genes were largely regulated by the actions of CCs on MGCs and the actions of MGCs on CCs. Especially, most cellular functional changes were regulated by bidirectional interactions (MGC⇔CC), including steroidogenesis, angiogenesis, COC expansion and EGFR signal transduction, which are well-known physiological phenomena in the ovulatory process [2, 26]. On the other hand, cellular functions such as follicle rupture and development were regulated by the actions of CCs on MGCs, while inflammatory response was regulated by the actions of MGCs on CCs. During the 4–12 h phase, the number of cellular functions regulated by bidirectional interactions decreased. Notably, steroidogenesis, COC expansion, and EGFR signal transduction were not identified as physiological phenomena regulated by the interactions. Physiological phenomena such as angiogenesis, follicle rupture, and inflammatory response remained activated by the actions of CCs on MGCs.

Figure 4B shows integrated data of cellular functional changes derived from downregulated genes and attenuated interactions. Few of the cellular functional changes were regulated by the attenuated interactions during the 0–4 h phase. During the 4–12 h phase, several cellular functions were identified as regulated by attenuated interactions. For example, steroidogenesis and EGFR were attenuated by bidirectional interactions, while COC expansion was attenuated by actions of CCs on MGCs. Oocyte maturation was regulated by attenuated actions of MGCs on CCs throughout the ovulation.

Figure 4C summarizes the time-dependent changes in interactions associated with well-known physiological phenomena in ovulation. Steroidogenesis, COC expansion, EGFR signaling were regulated by temporarily activated interactions, followed by attenuated interactions. On the other hand, angiogenesis, follicle rupture, and inflammatory response were regulated by continuously activated interactions throughout ovulation.

Validation of interactions between MGCs and CCs

To confirm our observations of mutual influences between MGCs and CCs, we established a novel coculture system of MGCs and COCs. Schematic diagrams of coculture experiments are shown in Fig. 5A. In this experiment, six cultures were established: COCs, COCs with hCG, COCs with hCG and MGCs, MGCs, MGCs with Areg and MGCs with Areg and COCs. After 12 h, we examined COC expansion and mRNA expression

A

Activated actions

Cellular function \ action	hCG 0h→4h			hCG 4h→12h		
	CC→MGC	MGC→CC	MGC⇄CC	CC→MGC	MGC→CC	MGC⇄CC
Steroidogenesis	○	○	○			
Angiogenesis	○	○	○	○		
Follicle rupture	○			○		
Inflammatory response		○		○		
COC expansion	○	○	○			
Endocytosis				○		
Lipid metabolism				○	○	○
Migration	○	○	○			
Cell cycle	○	○	○	○	○	○
Development	○					
EGFR signal transduction	○	○	○			
Other signal transduction					○	

B

Attenuated actions

Cellular function \ action	hCG 0h→4h			hCG 4h→12h		
	CC→MGC	MGC→CC	MGC⇄CC	CC→MGC	MGC→CC	MGC⇄CC
Steroidogenesis				○	○	○
COC expansion				○		
Oocyte maturation		○			○	
Endocytosis				○		
Migration				○	○	○
Cell cycle	○	○	○	○	○	○
EGFR signal transduction				○	○	○
Other signal transduction	○					

C

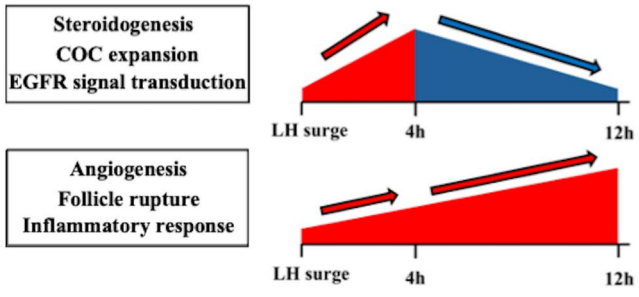

Fig. 4 (See legend on next page.)

(See figure on previous page.)

Fig. 4 Changes in cell-cell interactions and their association with physical phenomena during ovulation. Activated actions were linked to functional changes associated with upregulated genes, while attenuated actions were linked to functional changes associated with downregulated genes. Any actions of MGCs on CCs were considered to affect the cellular functions of CCs, while any actions of CCs on MGCs were considered to affect the cellular functions of MGCs. A circle in each column indicates the presence of an action that regulates the corresponding cellular function listed on the left. If circle appear in both the "CC→MGC" and "MGC→CC" columns for the same function, it represents the presence of a bidirectional interaction (MGC⇄CC). **A** Activated actions between MGCs and CCs regulating the cellular function. **B** Attenuated actions between MGCs and CCs regulating the cellular function. **C** Summary of time-course changes of interactions related to physiological phenomena. Activation of interactions were shown by red, and inactivation of interactions were shown by blue. The interactions associated with steroidogenesis, COC expansion, and EGFR signal transduction are temporary activated during the ovulatory process while those associated with angiogenesis, follicle rupture, and inflammatory response are continuously activated throughout the ovulatory process

of representative genes in CCs and mRNA expression of representative genes in MGCs. COC expansion was observed when COCs were cocultured with MGCs in the presence of hCG, but not when COCs were cultured without MGCs, either with or without hCG stimulation (Fig. 5B). These results indicated that our coculture system recapitulated the in vivo ovulatory process, by reproducing the interactions between MGCs to CCs. To identify the effects of interactions on representative cellular functions during ovulation, we used qRT-PCR to quantify the expression of marker genes of steroidogenesis, angiogenesis, follicle rupture, inflammatory response, and COC expansion. These functions were selected from those regulated by the activated interactions during ovulation (Fig. 4A). In CCs, the presence of MGCs significantly upregulated the expressions of genes related to steroidogenesis (*StAR*, *Cyp11a1*) [27], angiogenesis (*Vegfa*) [28], and COC expansion (*Has2*) [29] (Fig. 5C). Similarly, in MGCs, the presence of COCs significantly upregulated expressions of genes related to steroidogenesis (*StAR*, *Cyp11a1*) [27], angiogenesis (*Vegfa*) [28], COC expansion (*Tnfip6*) [30], follicle rupture (*Adamts1*) [31], inflammatory response (*Ptgs2*) [32] (Fig. 5D). In our preliminary experiment, coculture of MGCs with oocytes under Areg stimulation did not enhance Areg-induced gene expression in MGCs. Based on this, we considered that the synergistic effects observed in the coculture with COCs are mainly attributable to CCs rather than to factors secreted from the oocyte. Notably, marker genes of cellular functions regulated by bidirectional activated interactions (steroidogenesis, angiogenesis, and COC expansion) were significantly upregulated in both cell types (Fig. 5C, D), indicating that the activation of these cellular functions was bidirectional.

Discussion

In this study, we not only elucidated the dynamic changes in cellular functions of MGCs and CCs during ovulation (Fig. 2), but also revealed that cell-cell interactions between them regulate many physiological phenomena during ovulation (Fig. 4).

Although previous genome-wide analyses [1, 5] reported transcriptomic changes in MGCs and CCs during ovulation, each of them examined only one of the two cell types. In contrast, our genome-wide analysis simultaneously examined both MGCs and CCs isolated from the same follicle, enabling a direct comparison of their gene expression profiles under identical physiological conditions. This approach revealed that dynamic transcriptomic changes occur in both MGCs and CCs during ovulation, leading to dramatic changes in multiple cellular functions. Although MGCs and CCs are fundamentally distinct cell populations with different characteristics and roles [33], our analysis indicated that they also share cellular functions during ovulation. This is not surprising because hyaluronic acid production, which contributes to COC expansion, has been reported not only in CCs but also in MGCs during the early ovulatory phase [34]. Similarly, progesterone production, which is usually associated with MGCs, also occurs in CCs [35]. These findings suggest that while MGCs and CCs retain their cell-type–specific functions, they also exhibit overlapping functional changes, indicating coordinated but distinct contributions to the ovulatory process.

Simultaneous transcriptome analyses of MGCs and CCs provided a much better understanding of their interactions and physiological phenomena during ovulation. By synchronizing time-series transcriptome data from both cell types, we were able to identify cell-cell interactions and determined how these interactions contribute to specific changes in cellular function during ovulation. Previous studies have demonstrated the actions of MGCs on CCs. In response to the LH surge, MGCs secrete EGF-like factors, such as amphiregulin (Areg), which stimulate CCs and subsequently promote oocyte maturation and COC expansion [9]. In addition, the LH surge attenuates the interaction between natriuretic peptide precursor type C (NPPC) secreted by MGCs and natriuretic peptide receptor 2 (NPR2) expressed on CCs, leading to the resumption of oocyte meiosis, which is in a state of arrest prior to the LH surge [10]. In addition to these interactions, our study identified many novel actions of MGCs on CCs (Supplementary Table 5), including a novel action, Angptl2-ITGA5_ITGB1. Angptl2 has been reported to activate an inflammatory cascade in endothelial cells via integrin signaling and induce chemotaxis of monocytes/macrophages. Moreover, overexpressed Angptl2 in murine adipose tissue increased expression levels

of inflammatory cytokines (IL-6, TNF-α, IL-1β) within the tissue [25]. These findings suggest that Angptl2 secreted by MGCs could contribute to the regulation of inflammatory response in CCs. Furthermore, it should be noted that not only the actions of MGCs on CCs, but also many actions of CCs on MGCs were identified (Supplementary Table 5). For example, the Fgf2-Fgfr2 pathway was identified as a bidirectionally activated interaction. Fgf2 has been reported to promote progesterone production in buffalo luteal cells by upregulating the expression of StAR, Cyp11a1 and HSD3β [36]. Therefore, it is plausible that CCs regulate progesterone synthesis in MGCs through the Fgf2 secretion. Similarly, the Tgfb1-AVCR1_TGFbR pathway was identified as an interaction regulating angiogenesis, consistent with the angiogenetic role of Tgfb1 [37]. Angiogenesis during the ovulatory process has generally been considered to be regulated by Vegf secreted from MGCs [38]. Our analysis, however, suggests a possible additional mechanism whereby CCs indirectly contribute to follicular angiogenesis by secreting Tgfb1. These findings expand the current understanding of the cellular sources of angiogenic and steroidogenic signals during ovulation, highlighting a previously unrecognized role of CCs in coordinating both steroidogenesis and vascular changes within the follicle. Considering that the COC occupies a considerable part of the follicle, and both cell types can interact through follicular fluid, it is reasonable to assume that CCs can influence the cellular functions of MGCs during ovulation.

We showed the changes in interactions between CCs and MGCs and their association with physiological phenomena during ovulation. Not only actions of MGCs on CCs or CCs on MGCs, but also many bidirectional interactions were identified, particularly in the early phase of ovulation (0–4 h phase). This is consistent with our previous in silico analysis [11]. In other words, MGCs and CCs acquire similar cellular functions by mutually activating one another through bidirectional interactions.

Our results also showed that the physiological phenomena during ovulation are regulated by time-dependent activation and inactivation of the interactions between CCs and MGCs. For example, as shown in Fig. 4C, steroidogenesis (progesterone synthesis), COC expansion (hyaluronic acid production), and EGFR signal transduction (ERK 1/2 activation) are transiently activated during the early ovulatory phase due to the transient activation of cell-cell interaction. Previous studies have reported similar transient changes in physiological phenomena during ovulation. Regarding steroidogenesis, plasma progesterone levels rapidly increased after the LH surge, followed by a decline [4]. Similarly, hyaluronic acid production in the COC, which is related to COC expansion, was shown to transiently increase after the LH surge [39]. ERK1/2, a key downstream factor in EGFR signaling, was transiently activated in both MGCs and CCs after the LH surge [40, 41]. On the other hand, angiogenesis, follicle rupture, and inflammatory response are regulated by activated cell-cell interactions throughout ovulation. Our analysis further showed that this sustained activation was supported by the continued upregulation of genes such as *Angpl4* (angiogenesis) [42], *Edn2* (follicle rupture) [43], and *Il6* (inflammatory response) [44], suggesting that persistent gene upregulation keeps these cellular functions activated during ovulation. In fact, sustained activation of angiogenesis, follicle rupture and inflammatory response have been observed after the LH surge [2, 3, 16, 45]. Our study is the first to demonstrate that distinct patterns of cell-cell interactions regulate specific physiological phenomena during ovulation, depending on their timing and directionality.

A key strength of our study is the establishment of a novel coculture system for MGCs and COCs, enabling us to confirm their mutual influences. Genes associated with physiological phenomena regulated by bidirectional interactions, including steroidogenesis, angiogenesis, and COC expansion, were upregulated in both MGCs and CCs in response to their mutual presence (Fig. 5C and D), in agreement with the result of the interactome analysis (Fig. 4A). In addition to gene upregulation, COC expansion was observed in vitro only when MGCs were present. These results strongly suggest that our novel coculture system effectively recapitulates the in vivo ovulatory process.

A limitation of this study is that we did not prepare no-hCG–treated samples for RNA-seq analysis. Therefore, we cannot exclude the possibility that differential expression of some genes in MGCs and CCs was not due to hCG-induced ovulatory responses, but rather to time dependent effects. Another limitation of this study is the use of Areg to examine the action of CCs on MGCs in the in vitro experiment, because CCs do not respond to hCG due to very low levels of LH receptor. During the ovulatory process, Areg is secreted from MGCs after the LH surge and stimulates CCs [9]. The stimulated CCs then affect MGCs. Therefore, stimulation with Areg may only reflect partial (Areg-induced) ovulatory responses and may not fully recapitulate the in vivo sequence of events. Finally, although we demonstrated that COCs can influence gene expression in MGCs under Areg stimulation, we could not identify which specific factors secreted from COCs are responsible for these effects. Further studies will be needed to comprehensively characterize COC-derived factors and clarify their mechanistic contributions to MGC regulation during the ovulatory process.

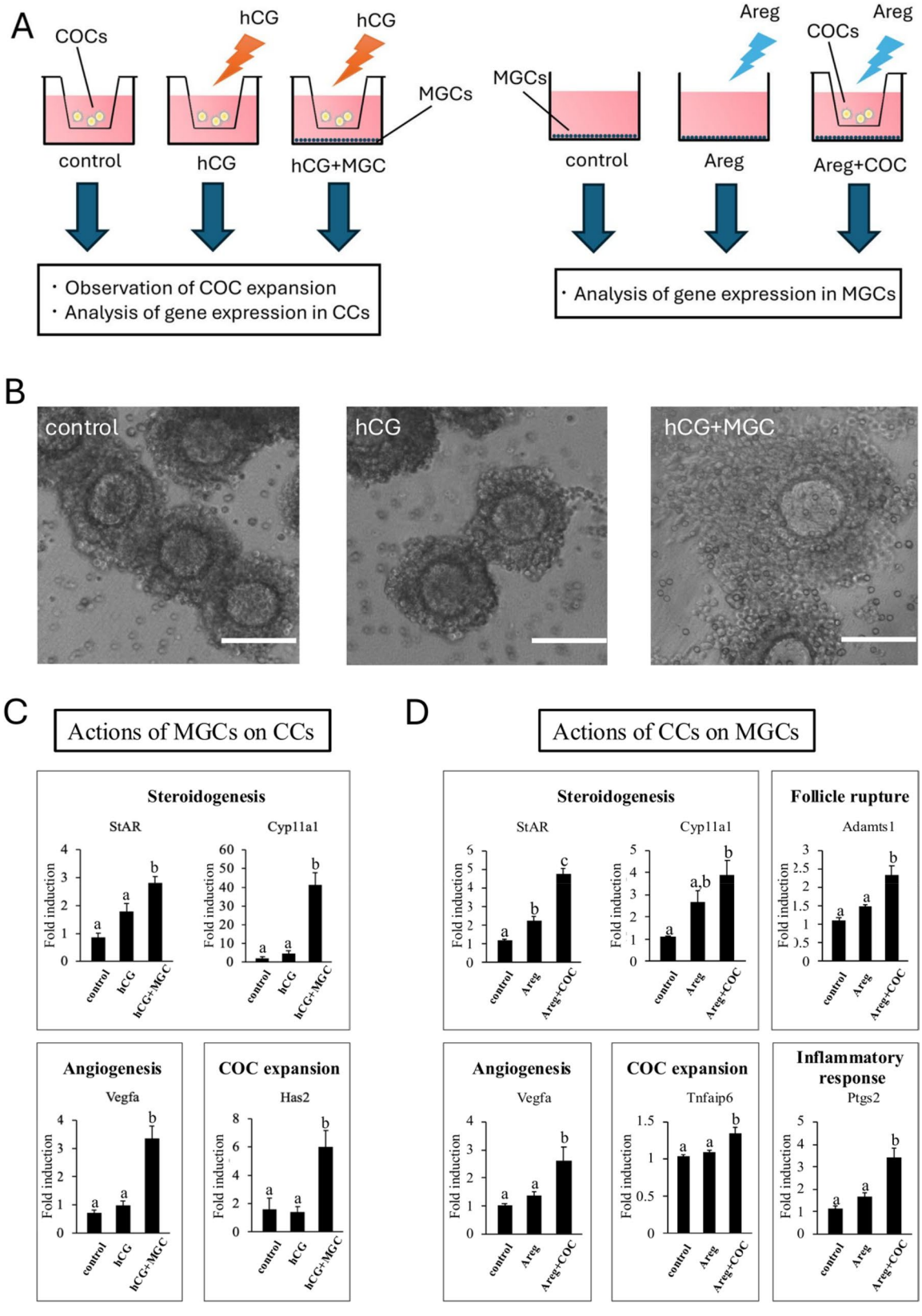

Fig. 5 (See legend on next page.)

(See figure on previous page.)

Fig. 5 Validation of interactions between MGCs and CCs by coculture system. **A** Schematic diagrams of coculture experiment. Left: To validate the actions of MGCs on CCs, COCs were cultured either without hCG (control), with hCG (hCG), or cocultured with MGCs in the presence of hCG (hCG + MGC). After 12 h, COC expansion and mRNA expression of representative genes in CCs were examined. Right: To validate the actions of CCs on MGCs, MGCs were cultured either without Areg (control), with Areg (Areg), or cocultured with COCs in the presence of Areg (Areg + COC). After 12 h, mRNA expression of representative genes in MGCs was examined. **B** Effect of MGCs on COC expansion. COC expansions was observed only when COCs were cocultured with MGCs in the presence of hCG. Scale bars: 100 µm. **C** Effect of actions of MGCs on CCs on gene expression in CCs. mRNA expression levels of representative genes in CCs, associated with specific cellular functions, were analyzed by qRT-PCR. Values are presented as mean ± SEM ($n = 3$ biological replicates). mRNA levels were normalized to *Gapdh* and expressed relative to one of the corresponding 0 h sample. Different superscript letters indicate significant difference ($P < 0.05$, one-way ANOVA followed by Tukey-Kramer test). **D** Effect of actions of COCs on MGCs on gene expression in MGCs. mRNA expression levels of representative genes in MGCs, associated with specific cellular functions, were analyzed by qRT-PCR. Values are presented as mean ± SEM ($n = 3$ biological replicates). mRNA levels were normalized to *Gapdh* and expressed relative to one of the corresponding 0 h sample. Different superscript letters indicate significant difference ($P < 0.05$, one-way ANOVA followed by Tukey-Kramer test)

Conclusions

During ovulation, dynamic interactions between MGCs and CCs within the follicle play a crucial role in coordinating various physiological phenomena. Our study is particularly valuable in uncovering the actions of CCs on MGCs, while previous studies have focused only on the actions of MGCs on CCs. In addition to providing comprehensive interaction profiling, our novel coculture system will contribute to elucidating the mechanisms underlining follicular events during ovulation.

Abbreviations

LH	Luteinizing hormone
MGCs	Mural granulosa cells
CCs	Cumulus cells
eCG	Equine chorionic gonadotropin
hCG	Human chorionic gonadotropin
COC	Cumulus-oocyte complex
Areg	Amphiregulin
NPPC	Natriuretic peptide precursor type C
NPR2	Natriuretic peptide receptor 2
qRT-PCR	Quantitative Reverse Transcriptase-Polymerase ChainReaction
RNA-seq	RNA sequencing
mRNA	Messenger RNA
DEGs	Differentially expressed genes
GO	Gene Ontology
REVIGO	Reduce and visualize gene ontology
FCS	Fetal calf serum
EGFR	Epidermal growth factorreceptor

Supplementary Information

The online version contains supplementary material available at https://doi.org/10.1186/s12958-025-01503-y.

Supplementary Material 1.

Supplementary Material 2.

Supplementary Material 3.

Supplementary Material 4.

Supplementary Material 5.

Supplementary Material 6.

Supplementary Material 7.

Supplementary Material 8.

Acknowledgements

Not applicable.

Authors' contributions

A.S., M.I., T.Y. and H.T.-K. conducted the experiment and collected data; A.S., I.T., T.F., T.T. and S.S. collected and analyzed the data; A.S., I.T. and Y.S. composed the manuscript; and A.S., I.T., and N.S. were responsible for the concept and study design. All authors contributed to the interpretation, discussion and editing of the manuscript. All authors have read and approved the manuscript.

Funding

This work was supported in part by JSPS KAKENHI (Grant Number 23K08824, 23K15838, 23K27734, 24K12533, 24K12579).

Data availability

Original data generated and analyzed during this study are included in this published article or in the data repositories listed in References. RNA-seq data are deposited in NCBI Gene Expression Omnibus (GEO) under accession number GSE301074 and are accessible at https://www.ncbi.nlm.nih.gov/geo/query/acc.cgi? acc=GSE301074 [46].The R scripts used for data analysis are available at the public GitHub repository: https://github.com/amon58/mural-granulosa-cumulus-interactions.

Declarations

Ethics approval and consent to participate

This study was reviewed and approved by the committee for ethics on animal experiment in Yamaguchi University Graduate School of Medicine.

Consent for publication

Not applicable.

Competing interests

The authors declare no competing interests.

Received: 18 August 2025 / Accepted: 19 November 2025
Published online: 25 November 2025

References

1. Shirafuta Y, Tamura I, Ohkawa Y, Maekawa R, Doi-Tanaka Y, Takagi H, et al. Integrated analysis of transcriptome and histone modifications in granulosa cells during ovulation in female mice. Endocrinology. 2021;162:bqab128.
2. Duffy DM, Ko C, Jo M, Brannstrom M, Curry TE. Ovulation: parallels with inflammatory processes. Endocr Rev. 2019;40:369–416.
3. Trau HA, Davis JS, Duffy DM. Angiogenesis in the primate ovulatory follicle is stimulated by luteinizing hormone via prostaglandin E2. Biol Reprod. 2015;92:15.
4. Tungmahasuk D, Fungbun N, Laoharatchatathanin T, Terashima R, Kurusu S, Kawaminami M. Effects of gonadotropin-releasing hormone agonist on human chorionic gonadotropin activity in granulosa cells of immature female rats. J Reprod Dev. 2018;64:129–34.
5. Hernandez-Gonzalez I, Gonzalez-Robayna I, Shimada M, Wayne CM, Ochsner SA, White L, et al. Gene expression profiles of cumulus cell oocyte complexes during ovulation reveal cumulus cells express neuronal and immune-related genes: does this expand their role in the ovulation process? Mol Endocrinol. 2006;20:1300–21.

6. Diaz FJ, Wigglesworth K, Eppig JJ. Oocytes determine cumulus cell lineage in mouse ovarian follicles. J Cell Sci. 2007;120:1330–40.
7. Eppig JJ, Wigglesworth K, Pendola F, Hirao Y. Murine oocytes suppress expression of luteinizing hormone receptor messenger ribonucleic acid by granulosa cells. Biol Reprod. 1997;56:976–84.
8. Liu J, Yao R, Lu S, Xu R, Zhang H, Wei J, et al. Synergistic effect between LH and estrogen in the acceleration of cumulus expansion via GPR30 and EGFR pathways. Aging (Albany NY). 2020;12:20801–16.
9. Park JY, Su YQ, Ariga M, Law E, Jin SL, Conti M. Egf-like growth factors as mediators of LH action in the ovulatory follicle. Science. 2004;303:682–4.
10. Zhang M, Su YQ, Sugiura K, Xia G, Eppig JJ. Granulosa cell ligand NPPC and its receptor NPR2 maintain meiotic arrest in mouse oocytes. Science. 2010;330:366–9.
11. Shirafuta Y, Tamura I, Shiroshita A, Fujimura T, Maekawa R, Taketani T, et al. Analysis of cell-cell interaction between mural granulosa cells and cumulus granulosa cells during ovulation using single-cell RNA sequencing data of mouse ovary. Reprod Med Biol. 2024;23:e12564.
12. Park CJ, Lin PC, Zhou S, Barakat R, Bashir ST, Choi JM, et al. Progesterone receptor serves the ovary as a trigger of ovulation and a terminator of inflammation. Cell Rep. 2020;31:107496.
13. Lee L, Asada H, Kizuka F, Tamura I, Maekawa R, Taketani T, et al. Changes in histone modification and DNA methylation of the StAR and Cyp19a1 promoter regions in granulosa cells undergoing luteinization during ovulation in rats. Endocrinology. 2013;154:458–70.
14. Okada M, Lee L, Maekawa R, Sato S, Kajimura T, Shinagawa M, et al. Epigenetic changes of the Cyp11a1 promoter region in granulosa cells undergoing luteinization during ovulation in female rats. Endocrinology. 2016;157:3344–54.
15. Doi-Tanaka Y, Tamura I, Shiroshita A, Fujimura T, Shirafuta Y, Maekawa R, et al. Differential gene expression in decidualized human endometrial stromal cells induced by different stimuli. Sci Rep. 2024;14:7726.
16. Shinagawa M, Tamura I, Maekawa R, Sato S, Shirafuta Y, Mihara Y, et al. C/EBPbeta regulates Vegf gene expression in granulosa cells undergoing luteinization during ovulation in female rats. Sci Rep. 2019;9:714.
17. Hayashi-Okada M, Sato S, Nakashima K, Sakai T, Tamehisa T, Kajimura T, et al. Identification of long noncoding RNAs downregulated specifically in ovarian high-grade serous carcinoma. Reprod Med Biol. 2024;23:e12572.
18. Tamura I, Miyamoto K, Hatanaka C, Shiroshita A, Fujimura T, Shirafuta Y, et al. Nuclear actin assembly is an integral part of decidualization in human endometrial stromal cells. Commun Biol. 2024;7:830.
19. Huang da W, Sherman BT, Lempicki RA. Systematic and integrative analysis of large gene lists using DAVID bioinformatics resources. Nat Protoc. 2009;4:44–57.
20. Supek F, Bosnjak M, Skunca N, Smuc T. REVIGO summarizes and visualizes long lists of gene ontology terms. PLoS One. 2011;6:e21800.
21. Jin S, Guerrero-Juarez CF, Zhang L, Chang I, Ramos R, Kuan CH, et al. Inference and analysis of cell-cell communication using CellChat. Nat Commun. 2021;12:1088.
22. Lacan A, Sebag M, Hanczar B. GAN-based data augmentation for transcriptomics: survey and comparative assessment. Bioinformatics. 2023;39:i111–20.
23. Satija R, Farrell JA, Gennert D, Schier AF, Regev A. Spatial reconstruction of single-cell gene expression data. Nat Biotechnol. 2015;33:495–502.
24. Emori C, Wigglesworth K, Fujii W, Naito K, Eppig JJ, Sugiura K. Cooperative effects of 17beta-estradiol and oocyte-derived paracrine factors on the transcriptome of mouse cumulus cells. Endocrinology. 2013;154:4859–72.
25. Tabata M, Kadomatsu T, Fukuhara S, Miyata K, Ito Y, Endo M, et al. Angiopoietin-like protein 2 promotes chronic adipose tissue inflammation and obesity-related systemic insulin resistance. Cell Metab. 2009;10:178–88.
26. Fan HY, Liu Z, Shimada M, Sterneck E, Johnson PF, Hedrick SM, et al. MAPK3/1 (ERK1/2) in ovarian granulosa cells are essential for female fertility. Science. 2009;324:938–41.
27. Stocco DM. The role of the star protein in steroidogenesis: challenges for the future. J Endocrinol. 2000;164:247–53.
28. Fraser HM, Wulff C. Angiogenesis in the corpus luteum. Reprod Biol Endocrinol. 2003;1:88.
29. Richards JS. Ovulation: new factors that prepare the oocyte for fertilization. Mol Cell Endocrinol. 2005;234:75–9.
30. Fulop C, Szanto S, Mukhopadhyay D, Bardos T, Kamath RV, Rugg MS, et al. Impaired cumulus mucification and female sterility in tumor necrosis factor-induced protein-6 deficient mice. Development. 2003;130:2253–61.
31. Russell DL, Brown HM, Dunning KR. ADAMTS proteases in fertility. Matrix Biol. 2015;44–46:54–63.
32. Dubois RN, Abramson SB, Crofford L, Gupta RA, Simon LS, Van De Putte LB, et al. Cyclooxygenase in biology and disease. FASEB J. 1998;12:1063–73.
33. Turathum B, Gao EM, Chian RC. The function of cumulus cells in oocyte growth and maturation and in subsequent ovulation and fertilization. Cells. 2021;10:2292.
34. Salustri A, Yanagishita M, Underhill CB, Laurent TC, Hascall VC. Localization and synthesis of hyaluronic acid in the cumulus cells and mural granulosa cells of the preovulatory follicle. Dev Biol. 1992;151:541–51.
35. Magnusson C, Billig H, Eneroth P, Roos P, Hillensjo T. Comparison between the progestin secretion responsiveness to gonadotrophins of rat cumulus and mural granulosa cells in vitro. Acta Endocrinol (Copenh). 1982;101:611–6.
36. Punetha M, Chouhan VS, Sonwane A, Singh G, Bag S, Green JA, et al. Early growth response gene mediates in VEGF and FGF signaling as dissected by CRISPR in corpus luteum of water buffalo. Sci Rep. 2020;10:6849.
37. Kuo SW, Ke FC, Chang GD, Lee MT, Hwang JJ. Potential role of follicle-stimulating hormone (FSH) and transforming growth factor (TGFbeta1) in the regulation of ovarian angiogenesis. J Cell Physiol. 2011;226:1608–19.
38. Guzman A, Hernandez-Coronado CG, Gutierrez CG, Rosales-Torres AM. The vascular endothelial growth factor (VEGF) system as a key regulator of ovarian follicle angiogenesis and growth. Mol Reprod Dev. 2023;90:201–17.
39. Thomas C, Marx TL, Penir SM, Schuh M. Ex vivo imaging reveals the spatiotemporal control of ovulation. Nat Cell Biol. 2024;26:1997–2008.
40. Shimada M, Umehara T, Hoshino Y. Roles of epidermal growth factor (EGF)-like factor in the ovulation process. Reprod Med Biol. 2016;15:201–16.
41. Okamoto A, Nakanishi T, Tonai S, Shimada M, Yamashita Y. Neurotensin induces sustainable activation of the ErbB-ERK1/2 pathway, which is required for developmental competence of oocytes in mice. Reprod Med Biol. 2024;23:e12571.
42. Le Jan S, Amy C, Cazes A, Monnot C, Lamande N, Favier J, et al. Angiopoietin-like 4 is a proangiogenic factor produced during ischemia and in conventional renal cell carcinoma. Am J Pathol. 2003;162:1521–8.
43. Ko CJ, Cho YM, Ham E, Cacioppo JA, Park CJ. Endothelin 2: a key player in ovulation and fertility. Reproduction. 2022;163:R71–80.
44. Tanaka T, Narazaki M, Kishimoto T. IL-6 in inflammation, immunity, and disease. Cold Spring Harb Perspect Biol. 2014;6:a016295.
45. Oakley OR, Kim H, El-Amouri I, Lin PC, Cho J, Bani-Ahmad M, et al. Periovulatory leukocyte infiltration in the rat ovary. Endocrinology. 2010;151:4551–9.
46. Shiroshita A, Tamura I, Ito M, Yoneda T, Takasaki-Kawasaki H, Fujimura T et al. Transcriptome analysis of mural granulosa cells and cumulus cells during ovulation in mouse ovary. Gene Expression Omnibus. 2025. https://www

Publisher's Note